"Flying Through" and "Flying Around" a PET/CT Scan: Pilot Study and Development of 3D Integrated ^{18}F-FDG PET/CT for Virtual Bronchoscopy and Colonoscopy

Andrew Quon, Sandy Napel, Christopher F. Beaulieu, and Sanjiv S. Gambhir

Molecular Imaging Program at Stanford, Departments of Radiology and Bioengineering, Stanford University, Stanford, California

The objective of this pilot project was to devise a new image acquisition and processing technique to produce PET/CT images rendered in 3-dimensional (3D) volume that can then be reviewed in several 3D formats such as virtual bronchoscopy and colonoscopy "fly-throughs" and external "fly-arounds." **Methods:** We tested the new imaging and processing protocol on 24 patients with various malignancies to determine whether it could dependably acquire and reformat standard tomographic 2-dimensional PET/CT images into 3D renderings. **Results:** This new technique added helpful information to the diagnostic interpretation for 2 of the 24 patients. Further, in the 6 patients undergoing mediastinoscopy, bronchoscopy, or endoscopy, 3D imaging helped in preprocedural planning. **Conclusion:** In this initial study, we demonstrated both the feasibility of rendering PET/CT images into 3D volumes and the potential clinical utility of this technique for diagnostic lesion characterization and preprocedural planning.

Key Words: PET/CT; FDG; fusion; virtual colonoscopy; virtual bronchoscopy; colon cancer; lung cancer

J Nucl Med 2006; 47:1081–1087

PET imaging performed with the radiolabeled glucose analog ^{18}F-FDG is useful for evaluating many types of malignancy because of its ability to image the level of glucose metabolism in suspected tumors (*1,2*). In particular, standard 2-dimensional (2D) tomographic ^{18}F-FDG PET and PET/CT are accurate for evaluating suggestive lung lesions, for staging mediastinal lung cancer metastases (*3–9*), and for evaluating colorectal cancer (*10–13*). However, the images still lack the exquisite anatomic information provided by the volume-rendered 3-dimensional (3D) images of multidetector CT.

Multidetector CT is capable of producing high-resolution 3D-volume datasets allowing for a multitude of viewing formats. Most commonly, these consist of multiplanar reformations based on transaxial data, but far more complex images are possible, such as external 3D renderings that allow viewers to "fly around" anatomic structures and internal 3D renderings that allow physicians to "fly through" luminal structures in a virtual endoscopy format (e.g., virtual bronchoscopy and virtual colonoscopy) (*14–24*).

To our knowledge, the 3D rendering of ^{18}F-FDG PET/CT images has not heretofore been reported. This report on our pilot study demonstrates the feasibility of producing 3D PET/CT images and describes the acquisition and processing protocols for 3D rendering of the central airways, mediastinum, and colon. We also show that the technique may potentially add important diagnostic information and aid in preprocedural planning.

MATERIALS AND METHODS

Patients

The pilot study looked at 24 patients referred for ^{18}F-FDG PET/CT to evaluate a previously diagnosed malignancy. The cancers of the patients were at various stages of management (Table 1). The distribution of malignancies among patients was as follows: lung cancer (8 cases), lymphoma (2 cases), colorectal cancer (5 cases), esophageal cancer (4 cases), breast cancer (2 cases), pancreatic cancer (1 case), cervical cancer (1 case), and head/neck cancer (1 case). The patient group consisted of 11 men and 13 women. Their ages ranged from 31 to 89 y (median, 64 y; mean, 63.3 y).

Twenty-one patients who underwent 3D PET/CT of the chest were initially referred by oncologists for a standard staging or restaging 2D ^{18}F-FDG PET/CT examination and separate contrast-enhanced CT of the chest. These patients were selected by the coordinator of this study on the basis of confirmed lung, mediastinal, hilar, or central airway disease that would be suitable for imaging with 3D PET/CT.

Three patients underwent PET/CT virtual colonoscopy. Two patients were referred to the study because an abnormal lesion that had been found on conventional colonoscopy required further evaluation (patients 22 and 23). These patients with known lesions served as the suitable baseline we needed to develop and evaluate

TABLE 1
Summary of Clinical Data, Imaging Findings, and Biopsy Results

Patient no.	Age (y)	Sex	PET/CT indication	SUV range of lesions	3D PET/CT helpful for radiologic interpretation?	Type of procedure performed after 3D PET/CT (if any)	3D PET/CT helpful for preprocedural planning?
1	86	M	Head/neck staging	4.3	No	Bronchoscopy	Yes
2	89	F	Esophageal staging	7.2−17.5	No	Mediastinoscopy	Yes
3	81	M	Lung restaging	5.3−8.4	No		
4	87	M	Lung staging	2.7−6.1	No	Mediastinoscopy	Yes
5	56	F	Lung staging	7.0−18.8	No		
6	72	F	Esophageal staging	3.8	Yes	Endoscopy	Yes
7	60	M	Esophageal staging	2.9−3.8	No	Mediastinoscopy	Yes
8	31	F	Breast staging	2.3	No		
9	61	F	Breast staging	2.6−3.8	No		
10	80	F	Lung staging	5.8−8.1	No		
11	65	F	Lung staging	3.2−5.1	No	Pneumonectomy	No
12	61	M	Esophageal restaging	2.9−4.8	No	Fine-needle aspiration	No
13	65	M	Lung staging	2.5−2.7	No		
14	52	F	Lymphoma staging	2.0	No		
15	65	M	Colorectal staging	1.8	No		
16	51	F	Colorectal staging	3.3	No	Mediastinoscopy	Yes
17	72	M	Lung staging	4.4	No	Pneumonectomy	No
18	52	F	Colorectal staging	3.9	No		
19	79	M	Lung staging	2.4−5.7	No	Pneumonectomy	No
20	40	F	Pancreatic restaging	2.8	No		
21	47	F	Cervical restaging	3.3	No		
22	37	M	Colorectal restaging*	5.6	No		
23	67	M	Colorectal staging*	12.1	No		
24	63	F	Lymphoma restaging*	4.5	Yes	Incomplete colonoscopy	Not applicable

*Patients 22−24 were prospectively recruited for virtual PET/CT colonoscopy after abnormal results on, or incomplete, conventional colonoscopy.

SUV = standardized uptake value.

the integrated PET/CT virtual colonoscopy acquisition protocol. We recruited 1 patient (patient 24) for PET/CT colonography without prior knowledge of any colonic abnormalities; in this patient, PET/CT was performed immediately before conventional colonoscopy.

All patients who underwent PET/CT virtual colonoscopy consented to the examination. Prior approval was obtained from the Investigational Review Board at Stanford University Medical Center.

Image Acquisition

The 24 patients were imaged on either a Discovery LS ($n = 4$) or a Discovery ST ($n = 20$) PET/CT scanner (GE Healthcare). All patients fasted for at least 12 h before intravenous injection of ^{18}F-FDG (370−666 MBq). Tracer uptake time ranged from 45 to 75 min. The scanning sequence consisted of unenhanced whole-body CT for attenuation correction of the PET images, followed by whole-body PET and then, in 21 of the 24 patients, by thin-slice contrast-enhanced chest CT. The scanning parameters for unenhanced whole-body CT included 140 kV, 80 mA, a 5.0-mm slice thickness, a pitch of 0.75:1, a 4.25-mm interval, and 15 mm per rotation. The PET scan was acquired in 2D mode, with 4 min per bed position and 6 or 7 bed positions total. Enhanced chest CT was performed with 75−150 mL of iodinated contrast material (Isoview; Amersham Health). For the Discovery LS, the parameters for enhanced chest CT were 120 kV, 300 mA, a 2.5-mm slice thickness, a 2.5-mm interval, a pitch of 1.5:1, and 4-detector mode. For the Discovery ST, the parameters were a 2.5-mm

collimation, a 1.25-mm overlap, 120 kV, 300 mA, a pitch of 1.5:1, 8-detector mode, and retrospective reconstruction to 1.25-mm slices. The detector configuration of the Discovery LS scanner was not capable of imaging with optimal overlap for 3D reformatting and therefore was suboptimal by current 3D CT reformatting standards; this suboptimal protocol was used on 4 of the 24 patients.

For the 3 patients referred for PET/CT virtual colonoscopy, the PET/CT colonography protocol was a specially designed modification of the CT colonography protocol used in the Stanford Radiology Department. This new protocol consisted of fasting and a bowel-cleansing regimen starting the afternoon before the day of the examination, similar to other CT colonography studies (25). ^{18}F-FDG (518−592 MBq) was administered intravenously, with a tracer uptake time of approximately 45 min. During both CT and PET, a Foley catheter was inserted into the rectum and air was insufflated into the colon using manual compression of a bulb at the end of the Foley catheter; the patient was given the bulb and asked to periodically reinsufflate his or her bowel at 30- to 45-s intervals during image acquisition. The entire scanning sequence consisted of prone CT, prone PET, a 2- to 3-min rest, supine CT, supine PET, and supine PET without air insufflation. Both prone and supine CT used the following parameters: a 2.5-mm collimation, a 1.25-mm overlap, 120 kV, 300 mA, 8-detector mode, and a pitch of 1.5:1. The PET scan was acquired in 2D mode in a total of 8 min (4 min per bed position and 2 bed positions total over the abdomen and pelvis).

Image Reconstruction and Reformatting

For all patients, 5 image sets were produced for physician review: standard 2D tomographic PET, standard 2D tomographic CT, standard 2D tomographic PET/CT, 3D-rendered external-perspective (fly-around) PET/CT, and 3D-rendered virtual endoluminal (fly-through) PET/CT.

For the standard 2D tomographic slices, PET images were reconstructed using iterative ordered-subset expectation maximization (26,27). Unenhanced CT images were reconstructed into 5-mm-thick sections, whereas contrast-enhanced images were reconstructed into 1.25- or 2.5-mm-thick sections (depending on whether the patient was imaged on the Discovery LS or the Discovery ST). These image sets were initially aligned on the Xeleris 1.1x workstation, which encoded the acquisition and reconstruction parameters (e.g., section location and spacing, in-plane pixel sizes) into the individual Digital Imaging and Communications in Medicine image headers to allow voxel-to-voxel correspondence between pairs of image volumes. When visual inspection revealed misalignment, such as that due to patient motion, the images were manually realigned with respect to pertinent nearby anatomic landmarks. PET and CT images in any plane either could be viewed separately or could be overlaid to place the PET intensity in the context of the anatomy imaged by CT.

Figure 1 summarizes the software-processing steps for both the 3D-rendered fly-around and virtual endoluminal views. For the 3D-ren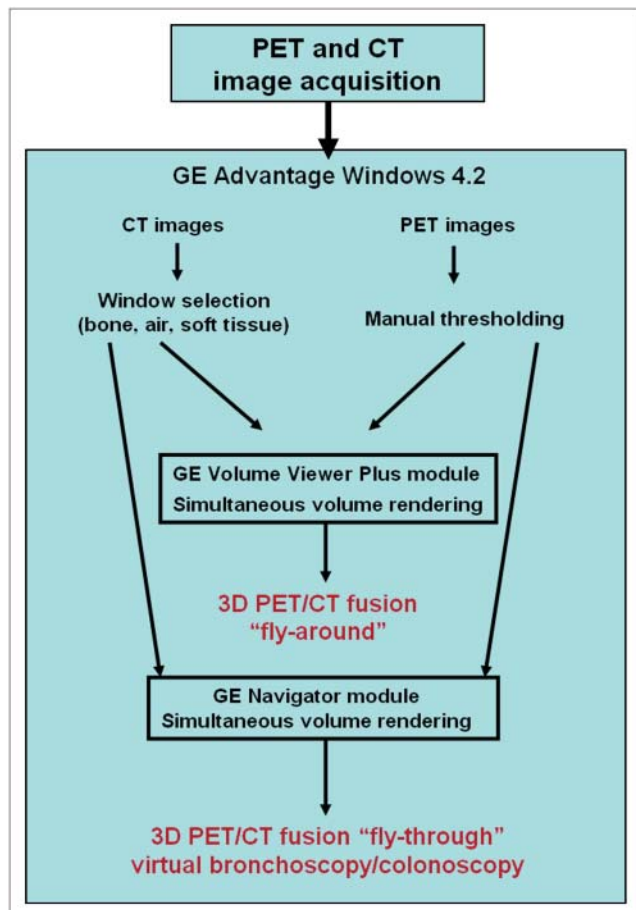dered fly-around views, we used the proprietary Volume Viewer Plus software (GE Healthcare) incorporated into the Advantage Windows platform (version 4.2; GE Healthcare), which provides various segmentation and editing operations allowing the user to isolate tissues of interest and then volume-renders (28) the CT volume (either unenhanced or contrast-enhanced) and the PET volume simultaneously. The resulting images can be viewed in arbitrary orientations in which the PET intensities appear in the proper 3D anatomic context, as given by the CT scan (Fig. 2).

For the 3D virtual endoluminal fly-through views, we used an early release of version 4.2 of the Advantage Windows Navigator software module provided to our 3D imaging laboratory by GE Healthcare. The standard software uses techniques commonly applied for clinical endoluminal imaging (23,24); for example, the air-filled tracheobronchial tree or colon is rendered by applying an opacity transfer function to the CT data that renders air transparent and soft-tissue walls opaque. This particular version additionally allows rendering of endoluminal views of combined PET and CT data (28) (Figs. 3B and 4E), with semitransparent airway or colon walls allowing PET intensities within the tissue to be viewed simultaneously.

Image Evaluation

In this proof-of-concept study, the potential added clinical value of 3D PET/CT images over standard 2D sliced images was evaluated and described.

Two physicians, a board-certified radiologist experienced in 3D imaging and a nuclear medicine physician experienced in PET/CT, reviewed the standard PET/CT images followed by the 3D-rendered PET/CT images. The interpreting physicians noted all abnormal foci not attributable to normal anatomic or physiologic ^{18}F-FDG uptake in order to assess the benefit of the 3D PET/CT images versus standard tomographs in specific categories of impact: changes in treatment regimen (surgical, chemotherapy,
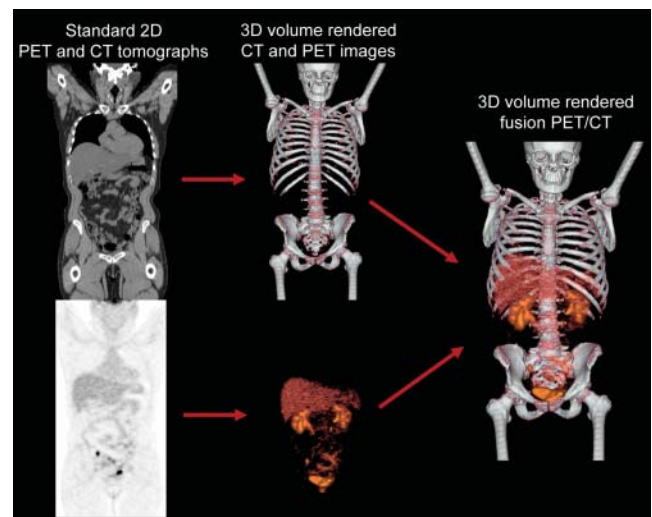

FIGURE 1. Flowchart of software-processing steps to produce 3D PET/CT images.

FIGURE 2. Schematic of 3D rendering of PET/CT images. Standard 2D tomographic CT and PET images, which contain scaling and alignment parameters calculated by software on PET/CT scanner, are simultaneously rendered (28) into single image that combines CT anatomy and PET activity in correct anatomic relationship. Bone, soft-tissue, and airway windows can be selected when using 3D rendering of CT to emphasize a particular anatomic perspective. Similar process is used to create 3D-rendered virtual endoscopy images.
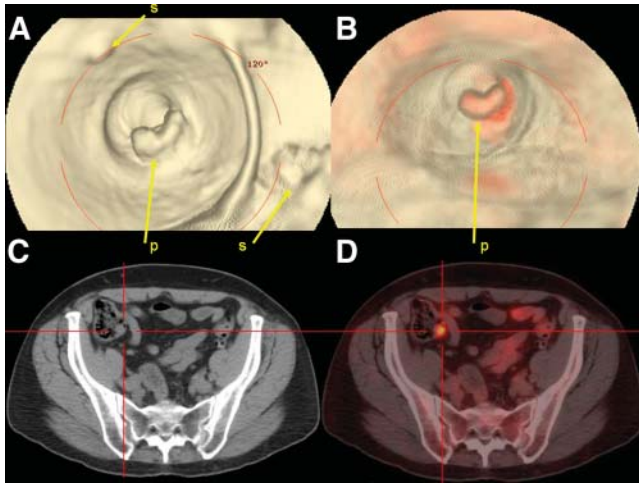
FIGURE 3. CT virtual colonoscopy compared with PET/CT virtual colonoscopy for detection of a potentially malignant lesion. (A) CT-based virtual colonoscopy showing several areas of stool that are difficult to distinguish from potential malignant polyp. (B) PET/CT virtual colonoscopy showing intense ^{18}F-FDG uptake that highlights suspected polyp relative to surrounding stool and greatly aids in differentiation of lesion from stool. (C and D) Retrospective review of standard 2D PET/CT tomographic slices reveals abnormal focus in colon that was missed on original interpretation (C) and would not have been detected without 3D fusion rendering (D). p = polyp; s = stool.

FIGURE 4. CT virtual bronchoscopy compared with PET/CT virtual bronchoscopy. (A, C, and E) Standard 2D PET/CT tomographs illustrating patient with highly ^{18}F-FDG–avid malignant subcarinal/paratracheal mass that extends along right tracheal sidewall and right bronchus. (B) CT virtual bronchoscopy illustrating that tracheal sidewall and carina appear normal, without indication of large tumors that abut central airways. (D) PET/CT virtual bronchoscopy showing abnormal ^{18}F-FDG uptake along right paratracheal wall, carina, and proximal right bronchus consistent with regions of malignant tissue that were not evident on CT virtual bronchoscopy. Images and video fly-through provided excellent preview of region before surgical bronchoscopy. t = tumor.

radiation therapy), changes in diagnostic strategies (e.g., performing or not performing a biopsy), and detection of previously undiagnosed lesions.

Additionally, a surgeon or interventional radiologist reviewed the 2D PET/CT tomographs and 3D image sets both before and after surgery, surgical endoscopy (mediastinoscopy, bronchoscopy, or colonoscopy), or percutaneous biopsy and assessed their usefulness in decisions on the type of procedure to perform (e.g., mediastinoscopy vs. bronchoscopy or percutaneous biopsy vs. surgical resection), in the selection of those lesions most amenable to biopsy, and in providing spatial localization to help guide the route or direction of the procedure.

RESULTS

Feasibility and Lesion Reproducibility of 3D PET/CT

An initial analysis of the fidelity of the 3D PET/CT technique was performed to confirm that all foci found on standard PET/CT could be faithfully reproduced and rendered into 3 dimensions. Table 1 catalogs all 24 patient cases, including the clinical indications, an account of each lesion, and the interpretation of these lesions before and after 3D rendering. All 42 foci that were originally detected on the 2D PET/CT tomographs could also be detected on the 3D-rendered PET/CT images by the interpreting radiologist and nuclear medicine physician. The standardized uptake value (29), a semiquantitative measure of tracer uptake in a tumor, ranged in intensity from 1.8 to 18.8 for the 42 visually detected foci. However, 1 additional suggestive lesion was detected on 3D PET/CT colonography
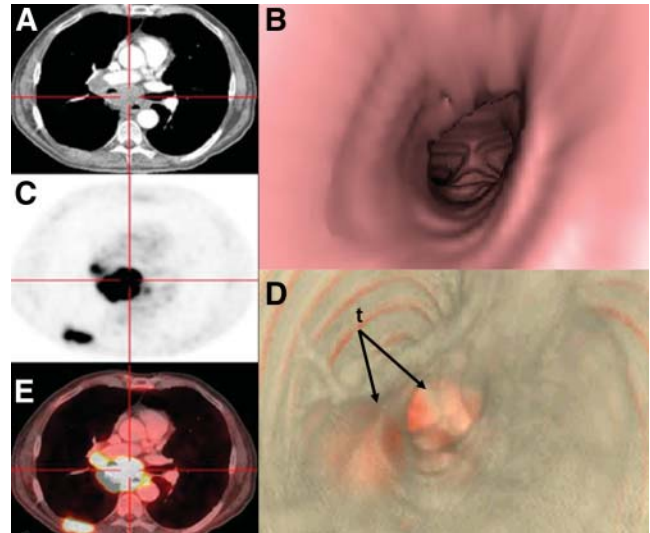
(patient 24) that was not initially detected on the original 2D PET/CT images.

Radiographic Characterization and Interpretation with 3D PET/CT

In their description of the added benefit of 3D PET/CT, the interpreting radiologist and nuclear medicine physician noted that the new technique appeared to aid in 2 of the 24 cases, allowing the detection of a possible second primary lesion in patient 24 and resulting in a switch from chemoradiation to surgical resection in patient 6.

In patient 24, who was 1 of the 3 patients undergoing PET/CT virtual colonoscopy, the CT portion of the examination was suboptimal because of the presence of a large amount of stool (from inadequate bowel cleansing). The 3D-rendered PET/CT scan clearly differentiated a polyp from fecal matter because the suspected polyp had intense ^{18}F-FDG uptake with a standardized uptake value of 7.8. In this patient, the lesion was overlooked on the original interpretation of the standard 2D PET/CT images and would not have been adequately evaluated by CT-based virtual colonoscopy alone because of the large amounts of fecal matter (Fig. 3; Supplemental Video 1 [all supplemental videos are available online at http://jnm.snmjournals.org]). Unfortunately, this site could not be examined histopathologically because the patient had an incomplete colonoscopy after imaging (because of the presence of

stool) and did not wish to undergo a repeated colonoscopy during treatment for her primary malignancy (lymphoma).

In patient 6, who had an elongated distal esophageal tumor with a narrow extension past the gastroesophageal junction and into the stomach, the initial interpretation was that the tumor was confined to the esophagus and that the stomach was inflamed. The 3D image obtained within a fly-around format clearly showed the direct extension of this tumor and ultimately led to a surgical proximal gastric resection rather than chemoradiation.

Preprocedural Planning with 3D PET/CT

The surgeons or interventional radiologists were surveyed as to the utility of the 3D technique for presurgical and preprocedural planning.

In total, 11 of the 24 patients underwent some type of procedure after 3D PET/CT. Six underwent bronchoscopy, endoscopy, or mediastinoscopy; 2 underwent percutaneous fine-needle aspiration of the lung; and 3 underwent surgical resection or exploration. The surveyed surgeons believed that 3D PET/CT aided in highlighting the location of lesions in all cases that required a subsequent endoscopic examination. Figure 5 and Supplementary Video 2 illustrate a case (patient 4) in which 2 suggestive lymph nodes requiring biopsy were noted in the peribronchial regions. Based partly on the 3D images, the surgeon selected mediastinoscopy over bronchoscopy (which was the original choice determined from 2D imaging). The 3D images also directed the route of the mediastinoscopy. Figure 4 and Supplementary Videos 3 and 4 demonstrate a case (patient 1) in which a large but complex mass abutted several portions of the carina, tracheal sidewall, and mainstem bronchi. The 3D PET/CT images helped highlight and direct bronchoscopic

FIGURE 5. 3D-rendered PET/CT fly-around aiding spatial localization of metastatic lymph nodes. (A, B, and D) Standard 2D tomographic ^{18}F-FDG PET/CT images illustrating abnormal focus in left side of mediastinum, posterior to left bronchus (demarcated by red cross-hairs). Despite coregistration of focus to contrast-enhanced thin-slice CT, it was difficult to detect and spatially localize lesion. (C) External 3D-rendered PET/CT fly-around showing abnormal ^{18}F-FDG PET focus hidden behind left mainstem bronchus, as well as several additional perihilar ^{18}F-FDG–avid lymph nodes. This image allowed clear spatial localization of lesion and guided mediastinoscopy biopsy. LN = lymph node.

biopsy to the multiple areas where the complex tumor directly contacted the central airway. However, the 3D PET/CT technique was not beneficial for planning of pneumonectomies in 3 patients or for planning of fine-needle aspiration biopsies of lung lesions in 2 patients.

Virtual Colonoscopy with PET/CT

Three of the 24 patients (patients 22−24) underwent PET/CT virtual colonoscopy using a new acquisition protocol specially designed within this study. The challenge in designing this protocol was to maintain anatomic coregistration of the bowel wall between the CT and PET portions of the examination. This proved to be difficult because traditional CT colonography requires insufflation of the colon with air and typically includes both prone and supine imaging (30). Air insufflation is particularly difficult with PET because the scanning time is severalfold longer than with CT. The 3 patients were scanned in both the prone and the supine positions, with and without bowel insufflation, during both the PET and the CT acquisitions.

Each of the 3 patients had a colon lesion that was used as a site of anatomic reference when the various image sets were compared. Two sets of virtual colonoscopy PET/CT images were reviewed: those with air insufflation and with the patient prone and those without air insufflation and with the patient supine. As demonstrated in Figure 6, which includes multiple views of the lesion of patient 23, prone
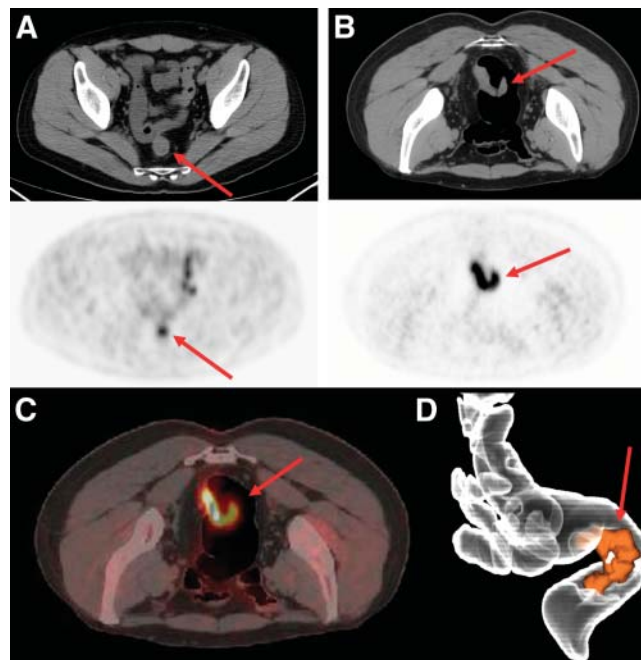

FIGURE 6. Virtual colonoscopy using supine and prone PET/CT with air insufflation. (A) Supine PET/CT without air insufflation showing abnormal focus (arrows) in rectosigmoid colon on PET. (B) Prone PET and CT with air insufflation providing excellent definition of same lesion shown in A on both PET and CT images. (C) PET/CT without air insufflation illustrating good image and lesion (arrow) coregistration. (D) 3D-rendered PET/CT colonography demonstrating lesion in its entirety.

images with air insufflation appeared to better define the lesion on both PET and CT images. Further, it appeared from these 3 patients that air insufflation during the 8-min PET acquisition is feasible (albeit with moderate patient discomfort) and allows for adequate anatomic coregistration between PET and CT.

DISCUSSION

This pilot study demonstrated for, what is to our knowledge, the first time that it is possible to generate 3D PET/CT images for fly-through and fly-around viewing. Three-dimensional fusion appears to have potential for presurgical visualization, particularly in guiding biopsies performed via endoscopy, mediastinoscopy, or bronchoscopy. This technique may also provide helpful information for radiologic interpretation, as was found in 2 of the 24 patients.

The 3 cases in which PET/CT virtual colonoscopy was used demonstrated the practicability of the integrated PET/CT colonography acquisition protocol developed in this study. Our initial experience with this technique has indicated that prone PET/CT acquisition with air insufflation provides the better image quality, and future protocols may be modified to omit supine acquisitions to minimize patient discomfort and shorten imaging time. Further, the diagnostic value of this type of imaging was demonstrated in the case in which 3D imaging revealed a polypoid lesion that had escaped detection on traditional tomographic PET, CT, and PET/CT. This case illustrated the potential synergistic enhancement of both PET and CT when rendered into 3 dimensions.

Limitations of this initial pilot study included the relatively few patients, the mixture of malignancies, and the variety of clinical stages. Also, not all lesions detected could undergo histopathologic analysis, nor was the effect of size on lesion detectability analyzed. Clearly, this project was a proof of concept rather than a validation of the technique. Despite these limitations, the initial findings are exciting and provide the impetus for future validation studies in controlled experiments. Future use of this technique may be expanded to include tracers other than ^{18}F-FDG and anatomic regions other than the chest and colon.

CONCLUSION

This pilot study demonstrated practicable acquisition and processing protocols designed to generate 3D-rendered PET/CT images, including fly-through virtual bronchoscopy and colonoscopy images and fly-around external 3D renderings. Previously, these detailed anatomic renderings were achievable with conventional imaging but not with PET. Additionally, this technique appears to show potential for guiding surgical procedures and for adding important diagnostic information that may herald new applications for the use of PET/CT.

REFERENCES

1. Gambhir S. Molecular imaging of cancer with positron emission tomography. *Nat Rev Cancer.* 2002;2:683–693.
2. Coleman RE. Clinical PET in oncology. *Clin Positron Imaging.* 1998;1: 15–30.
3. Pieterman RM, van Putten JW, Meuzelaar JJ, et al. Preoperative staging of non-small-cell lung cancer with positron-emission tomography. *N Engl J Med.* 2000;343:254–261.
4. Lardinois D, Weder W, Hany TF, et al. Staging of non-small-cell lung cancer with integrated positron-emission tomography and computed tomography. *N Engl J Med.* 2003;348:2500–2507.
5. Brink I, Schumacher T, Mix M, et al. Impact of [18F]FDG-PET on the primary staging of small-cell lung cancer. *Eur J Nucl Med Mol Imaging.* 2004;31: 1614–1620.
6. Schumacher T, Brink I, Mix M, et al. FDG-PET imaging for the staging and follow-up of small cell lung cancer. *Eur J Nucl Med.* 2001;28:483–488.
7. Gould MK, Maclean CC, Kuschner WG, Rydzak CE, Owens DK. Accuracy of positron emission tomography for diagnosis of pulmonary nodules and mass lesions: a meta-analysis. *JAMA.* 2001;285:914–924.
8. Herder GJ, Golding RP, Hoekstra OS, et al. The performance of (18)F-fluorodeoxyglucose positron emission tomography in small solitary pulmonary nodules. *Eur J Nucl Med Mol Imaging.* 2004;31:1231–1236.
9. Shim SS, Lee KS, Kim BT, et al. Non-small cell lung cancer: prospective comparison of integrated FDG PET/CT and CT alone for preoperative staging. *Radiology.* 2005;236:1011–1019.
10. Kantorova I, Lipska L, Belohlavek O, Visokai V, Trubac M, Schneiderova M. Routine (18)F-FDG PET preoperative staging of colorectal cancer: comparison with conventional staging and its impact on treatment decision making. *J Nucl Med.* 2003;44:1784–1788.
11. Lonneux M, Reffad AM, Detry R, Kartheuser A, Gigot JF, Pauwels S. FDG-PET improves the staging and selection of patients with recurrent colorectal cancer. *Eur J Nucl Med Mol Imaging.* 2002;29:915–921.
12. Kalff V, Hicks RJ, Ware RE, Hogg A, Binns D, McKenzie AF. The clinical impact of (18)F-FDG PET in patients with suspected or confirmed recurrence of colorectal cancer: a prospective study. *J Nucl Med.* 2002;43:492–499.
13. Whiteford MH, Whiteford HM, Yee LF, et al. Usefulness of FDG-PET scan in the assessment of suspected metastatic or recurrent adenocarcinoma of the colon and rectum. *Dis Colon Rectum.* 2000;43:759–767.
14. Boiselle PM, Reynolds KF, Ernst A. Multiplanar and three-dimensional imaging of the central airways with multidetector CT. *AJR.* 2002;179:301–308.
15. Paik DS, Beaulieu CF, Jeffrey RB, Rubin GD, Napel S. Automated flight path planning for virtual endoscopy. *Med Phys.* 1998;25:629–637.
16. Laghi A, Iannaccone R, Carbone I, et al. Detection of colorectal lesions with virtual computed tomographic colonography. *Am J Surg.* 2002;183:124–131.
17. Laghi A, Iannaccone R, Carbone I, et al. Computed tomographic colonography (virtual colonoscopy): blinded prospective comparison with conventional colonoscopy for the detection of colorectal neoplasia. *Endoscopy.* 2002;34: 441–446.
18. Burke AJ, Vining DJ, McGuirt WF Jr, Postma G, Browne JD. Evaluation of airway obstruction using virtual endoscopy. *Laryngoscope.* 2000;110:23–29.
19. Vining DJ, Liu K, Choplin RH, Haponik EF. Virtual bronchoscopy: relationships of virtual reality endobronchial simulations to actual bronchoscopic findings. *Chest.* 1996;109:549–553.

20. Remy-Jardin M, Remy J, Artaud D, Fribourg M, Duhamel A. Volume rendering of the tracheobronchial tree: clinical evaluation of bronchographic images. *Radiology.* 1998;208:761–770.

21. Remy-Jardin M, Remy J, Artaud D, Fribourg M, Naili A. Tracheobronchial tree: assessment with volume rendering—technical aspects. *Radiology.* 1998;208: 393–398.

22. Rapp-Bernhardt U, Welte T, Doehring W, Kropf S, Bernhardt TM. Diagnostic potential of virtual bronchoscopy: advantages in comparison with axial CT slices, MPR and mIP? *Eur Radiol.* 2000;10:981–988.

23. Beaulieu CF, Rubin GD. Perspective rendering and virtual endoscopy. In: Fishman EK, Jeffrey RB Jr, eds. *Multidetector CT: Principles, Techniques, and Clinical Applications.* Boston, MA: Lippincott-Raven; 2004:35–52.

24. Rubin GD, Beaulieu CF, Argiro V, et al. Perspective volume rendering of CT and MR images: applications for endoscopic imaging. *Radiology.* 1996;199: 321–330.

25. Macari M, Bini EJ. CT colonography: where have we been and where are we going? *Radiology.* 2005;237:819–833.

26. Riddell C, Carson RE, Carrasquillo JA, et al. Noise reduction in oncology FDG PET images by iterative reconstruction: a quantitative assessment. *J Nucl Med.* 2001;42:1316–1323.

27. Lonneux M, Borbath I, Bol A, et al. Attenuation correction in whole-body FDG oncological studies: the role of statistical reconstruction. *Eur J Nucl Med.* 1999;26:591–598.

28. Cai W, Sakas G. Data intermixing and multi-volume rendering. *Comput Graph Forum.* 1999;18:359–368.

29. Strauss LG, Conti PS. The applications of PET in clinical oncology. *J Nucl Med.* 1991;32:623–648.

30. Yee J, Kumar NN, Hung RK, Akerkar GA, Kumar PR, Wall SD. Comparison of supine and prone scanning separately and in combination at CT colonography. *Radiology.* 2003;226:653–661.